Available online at www.pelagiaresearchlibrary.com

Pelagia Research Library

Advances in Applied Science Research, 2015, 6(3): 142-148

Pelagia Research Library

ISSN: 0976-8610
CODEN (USA): AASRFC

First-principle study of magnetism in B-doped ZnO with GGA and GGA+*U*

Yousif Shoaib Mohammed[1,2,3]

[1]*Department of Physics, College of Science & Art, Qassim University, Oklat Al- Skoor, Saudi Arabia*
[2]*Department of Physics, University of Dalanj, Dalanj, Sudan*
[3]*African City for Technology, Khartoum, Sudan*

ABSTRACT

First-principles calculations are performed to study the electronic structures and magnetic properties of nonmagnetic B-doped ZnO. We investigate the following three cases: (i) single B atom substituted at Zn site, (ii) single B atom substituted at O site, and (iii) two B atoms substituted at O sites. Both generalized gradient approximation (GGA) and GGA+U calculations show that a substitutional B atom at Zn sites is non-magnetic. While a substitutional B atom at O site introduces magnetic moment of about 3.0 μB, respectively. The magnetic moment mainly comes from the partially occupied 2p orbitals of substitutional B, its nearest neighboring Zn and second neighboring O atoms, and the biggest atomic moment is of B. The U correction for the 3d Zn and for the 2p O and B states obviously changes the magnetic moment of the B atom. Total energy calculations show that the antiferromagnetic (AFM) state is predicted to be the ground state for all configuration systems.

Key words: Zinc oxide; Boron-doping; Antiferromagnetic; GGA; GGA+U; DOS.

INTRODUCTION

Diluted magnetic semiconductors (DMSs) have attracted a great deal of attention because of the possibility of incorporating magnetic degrees of freedom in traditional semiconductors [1, 2]. DMSs are semiconductors which contain some magnetic atoms as impurities. They have the possibility to create functional material using the carrier control techniques in semiconductors. They are widely used in high- and low-tech applications such as, solar cells, heaters, defrosters, and optical coatings [3]. Ferromagnetism in diluted magnetic semiconductors is one of the interesting problems of this century in condensed matter physics [4 - 6].

Room temperature ferromagnetism has been reported by many researchers, such as TM doped ZnO [7 - 10], SnO_2 [11, 12], In_2O_3 [13, 14]. Interestingly, non-magnetic ion doped ZnO thin films also reveal robust ferromagnetism, e.g. nitrogen doped ZnO thin films [15 - 18], Carbon implanted ZnO [19] and Phosphorus doped ZnO [20]. The mechanism behind the enhancement of ferromagnetism by the doped nitrogen, carbon or phosphorus is still unclear. Some researchers believe that the magnetic mechanism of non-magnetic ion doped thin films of transition metal oxide comes from the localized states of oxygen defects [21, 22], which is different from the bound magnetic polaron (BMP) mechanism proposed by Coey [23] for magnetic ion doped transition metal oxides.

In addition to the technological appeal of room-temperature ferromagnetism in ZnO-based DMSs, ZnO offers other desirable features as a semiconductor host. Its strong piezoelectricity [24] is exploited in a variety of transducer applications [25] and has possible application in polarization field effect transistors [26]. The nonstoichiometric un-doped ZnO thin films usually show an n-type material with low resistivity due to the oxygen vacancies and zinc interstitials [27, 28]. Also long spin coherence times, with potential spintronic applications, have recently been reported at room temperature in n-type ZnO [29].

The structural, electrical and optical properties of B-doped ZnO films (ZnO:B), are widely studied [30 - 32]. Furthermore, Low-resistivity and high-stability ZnO films were grown by photo-atomic layer deposition (photo-ALD) technique using boron as an n-type dopant [33].

To our knowledge, there is no experimental study on the magnetic properties of nonmagnetic anion B-doped ZnO. In order to explore possible magnetic properties of B-doped ZnO, we investigate the effects of nonmagnetic B dopants on the electronic structures and magnetic properties of B-doped ZnO by first principles calculations.

COMPUTATIONAL METHOD

The calculations have been performed using Vienna ab-initio simulation package (VASP) [34, 35]. The B-doped ZnO system was modeled with a supercell built of 3×3×2 wurtzite unit cells, which is sufficient to avoid the interaction of the B atom with its images in neighboring supercells. (see Fig. 1). The exchange-correlation potential is treated with the generalized gradient approximation (GGA) [36] and the strong correlation effects are introduced by means of GGA+*U* scheme [37, 38]. The projector augmented wave potentials (PAW) were used for electron-ion interaction [39]. An energy cutoff of 400 eV was used for the plane wave expansion of the electronic wave function. Special *k* points were generated with a 3x3x2 grid based on the Monkhorst-Pack scheme [40]. It is known that local density approximation (LDA) or GGA suffers from underestimation of the band gap and an improper description of strongly localized electrons occupying the Zn 3d states for ZnO. Incorporating of on-site Coulomb interaction between the Zn 3d electrons into the LDA (LDA+*U*) or GGA (GGA+*U*) can give improved results [41, 42]. In the GGA+*U* calculations, the effective interaction parameter for Zn 3d states is set to *U*-*J*=7.0 eV, which is almost the same as the value used in Refs. [41, 43]. While for anion-2p states is taken as *U*=5.6 eV and *J*=1.2 eV for O 2p and B 2p, respectively, which is almost the same as the value used in Refs. [44] and [45] and is close to the estimated values from spectroscopic measurements in oxides [46, 47].

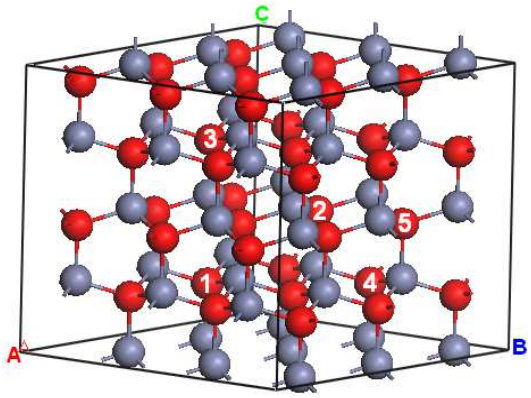

Fig. 1. (Color online) The 3x3x2 supercell of ZnO wurtzite consisting of 36 Zn and 36 O atoms. The gray atoms are Zn and the red atoms are O. The positions of B substituted by Zn and O are denoted by 0, and 1 - 5, respectively

The structure of B-doped ZnO was fully relaxed in our calculations and good convergence was obtained with energy and force at 10^{-4} eV and 10^{-2} eV/Å, respectively. We have also optimized the ratio of the lattice constants (*c/a*) at each volume by performing calculations for several different values of *c/a*. The calculated total energies as a function of volume were fitted to the Birch–Murnaghan equation of state (EOS) [48 - 51] to obtain equilibrium lattice constant *a*, the bulk modulus *B*0 and its pressure derivatives B_0'.

RESULTS AND DISSCUSSION

Table 1, shows the calculated lattice constants (*a* and *c)*, the *c/a* ratio, the bulk modulus B_0 and its pressure derivatives B_0', for undoped ZnO compared with experimental and previous calculation values [10, 41, 52 – 56]. From table 1, we find that the experimental value of *a* lies in between the GGA and GGA+*U* values, and the value of *c/a* is close to the GGA value. For all calculations we kept the lattice parameters *a* and *c* fixed at our calculated values for undoped ZnO as (3.29 and 5.28 Å) for GGA and (3.21 and 5.104 Å) for GGA+*U* respectively.

Table 1. *Calculated* structural parameters of wurtzite-ZnO compared with both experimental and theoretical data [10, 41, 52 - 56]. The table lists the calculated values for the lattice parameters *a* and *c* (in Å) at Zero-Pressure, the *c/a* ratio, the bulk modulus B_0 (in GPa) and its pressure derivative B_0' . for GGA and GGA+*U* respectively (GGA+*U* are in parenthesis)

Method	*a* (Å)	*c* (Å)	*c/a*	*B0 (GPa)*	B_0'	References
Theor.	3.29	5.28	1.605	144.6	4.6	This work
	(3.21)	(5.104)	(1.59)	(137.9)	(4.05)	
Theor.	3.29	5.284	1.606			10
	(3.19)	(5.149)	(1.614)			
Theor.	3.283	5.289	1.611	149		40
	(3.196)	(5.133)	(1.606)	(136)		
Theor.	3.29	5.241	1.593			51
Theor.	3.262	5.226	1.602			52
Theor.	3.199	5.163	1.6138	162.3	4.05	53
Expt.	3.2496	5.2042	1.6018	183	4	54
Expt.	3.2498	5.2066	1.6021	143	3.6	55

The cases of isolated B substitution on the Zn and O sites in $Zn_{36}O_{36}$ 3x3x2 supercell is first investigated (Fig. 1. Site 0 and 1), respectively. The corresponding concentration of B dopant is 2.8 at.%. The calculations show that the single B atom substituted at Zn site is non-magnetic, and the total energies of the supercell for GGA, GGA+U_{Zn} and GGA+U_O+U_B are listed in table 2. For the B atom substituted at O site, due to the larger atomic radius of B atom, the Zn and O atoms around B dopant move outward and the displacement is not isotropic. The total energy of spin polarized state calculated by the GGA, GGA+U_{Zn} and GGA+U_O+U_B is lower than that of non-spin-polarized state by 55.73, 98.09 and 80.92 meV, respectively, which indicates that the ground state of B atom substituted at O site in ZnO is magnetic. The GGA, GGA+U_{Zn} and GGA+U_O+U_B calculations show that the value of the magnetic moment of the supercell is about 3.0 μB for all approximations, and the most of it is located on the B atom, its four nearest neighboring Zn atoms and 12 second neighboring O atoms.

Table 2. The total energies of the supercell (*E*) for single B atom at Zn site calculated by GGA, GGA+U_{Zn} and GGA+U_O+U_B, respectively

	E (eV)
GGA	-332.2766
GGA+U_{Zn}	-328.3938
GGA+U_O+U_B	-213.2535

Table 3 lists the magnetic moment distribution calculated by the GGA, GGA+U_{Zn} and GGA+U_O+U_B. It is noted that the magnetic moment in B-doped ZnO is mainly contributed by the B atom, its nearest neighboring Zn atoms and its second neighboring O atoms and the biggest atomic moment is of B, which is similar to the result of N-doped ZnO [18], C-doped ZnO [19] and P-doped ZnO [20]. The *U* correction for Zn 3d states makes the magnetic moment of B atom bigger.

Table 3. The magnetic moment of the B atom (M_B), its four nearest neighboring Zn atoms (M_{Zn}) and 12 second neighboring O atoms (M_O) calculated by GGA, GGA+U_{Zn} and GGA+U_O+U_B, respectively

	M_B (μB)	M_{Zn} (μB)	M_O (μB)
GGA	0.740	0.616	0.533
GGA+U_{Zn}	0.837	0.623	0.480
GGA+U_O+U_B	0.744	0.652	0.594

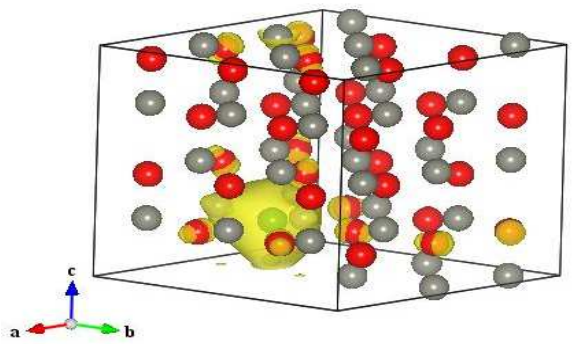

Fig. 2. (Color online) The spin density distribution in the relaxed 3×3×2 supercell containing a substitutional B atom calculated by GGA+U_{Zn}. Yellow isosurfaces represent spin densities. The red, gray and green balls represent O, Zn and B atoms, respectively

Fig. 2 shows the spin density distribution in the relaxed supercell calculated by GGA+U_{Zn}. The distribution in Fig. 2 reveals that the spin density of B atom is the biggest and the four nearest neighboring Zn atoms and 12 second neighboring O atoms are also slightly polarized. Furthermore, the spin density of the Zn and O atoms around B dopant unequally distribute. The spin density distribution calculated by GGA and GGA+U_O+U_B are almost same as distribution by GGA+U_{Zn}.

Figs. 3(a), (b) and (c) show the total density of states (DOS) of B-doped ZnO along with the partial DOS of 2p states of B atom, 3d states of a nearest neighboring Zn atom and 2p states of a second neighboring O atom calculated by GGA, GGA+U_{Zn} and GGA+U_O+U_B, respectively. It can be seen that the B substitution creates the spin splitting impurity states just above the top of the valence band, so substitutional B dopant can induce the ZnO to p-type semiconductor. Fermi level pass through the spin-down impurity states, which indicates that the system is half metallic. The spin-up impurity states are fully occupied but the spin-down states are partially filled. The impurity states are mostly formed by p states of B atom and the 3d states of nearest neighboring Zn atoms, whereas contribution of p states of second neighboring O atoms is minor. Therefore, the magnetic moment mainly comes from partially filled p orbitals of B atom and its nearest neighboring Zn atoms. Comparing Figs. 3(a), (b) and (c) one can see that the addition of U_{Zn} lead to downward shift of the Zn 3d states, which weakens the hybridization of the Zn 3d and O 2p states, while the addition of U_O+U_B remain the states constant. The impurity states near the Fermi level remains almost the same. Accordingly, the magnetic moment and its distribution calculated by the GGA, GGA+U_{Zn} and GGA+U_O+U_B are almost the same.

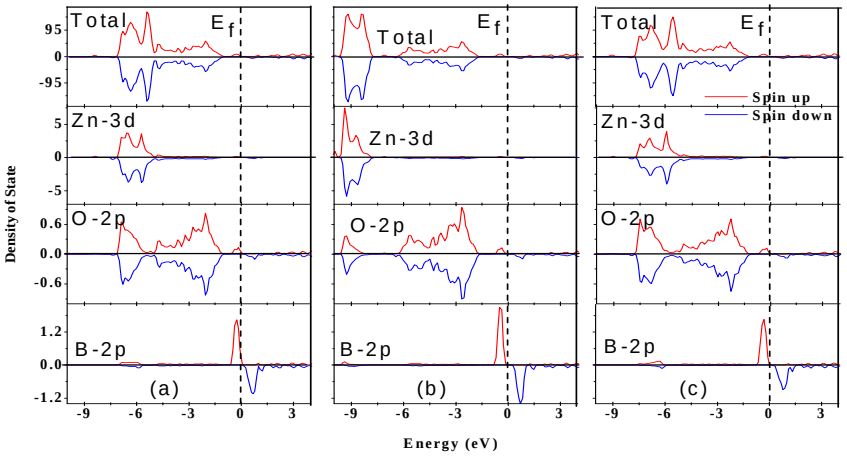

Fig. 3. (Color online) Total and partial DOS of a B substitution on the O site in the supercell calculated by (a) GGA, (b) GGA+U_{Zn}, and (c) GGA+U_O+U_B respectively. The Fermi energy is indicated by the dashed vertical line

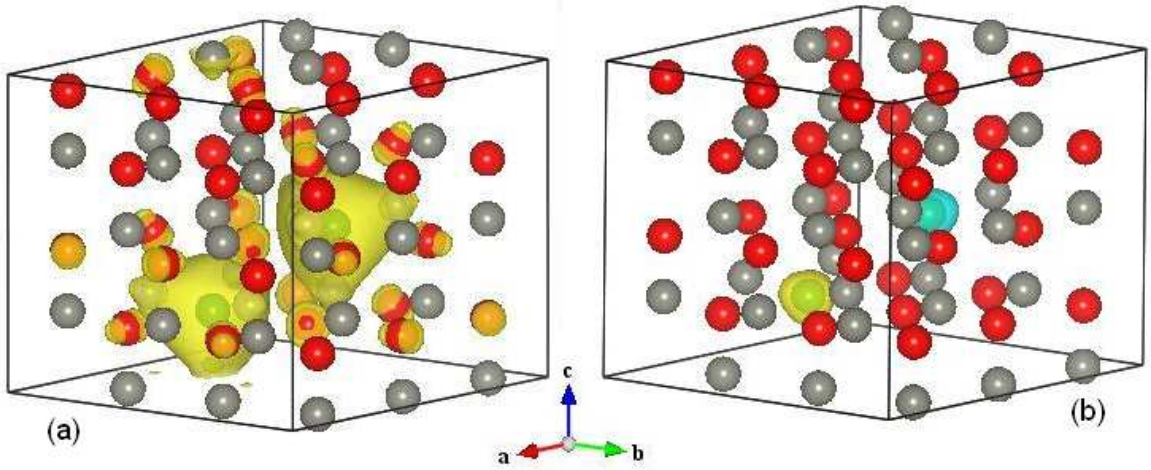

Fig. 4. (Color online) The spin density distribution in the relaxed 3×3×2 supercell containing a substitutional two B atom of B12 configuration calculated by GGA+U_{Zn}. Yellow isosurfaces represent spin densities. The red, gray and green balls represent O, Zn and B atoms, respectively

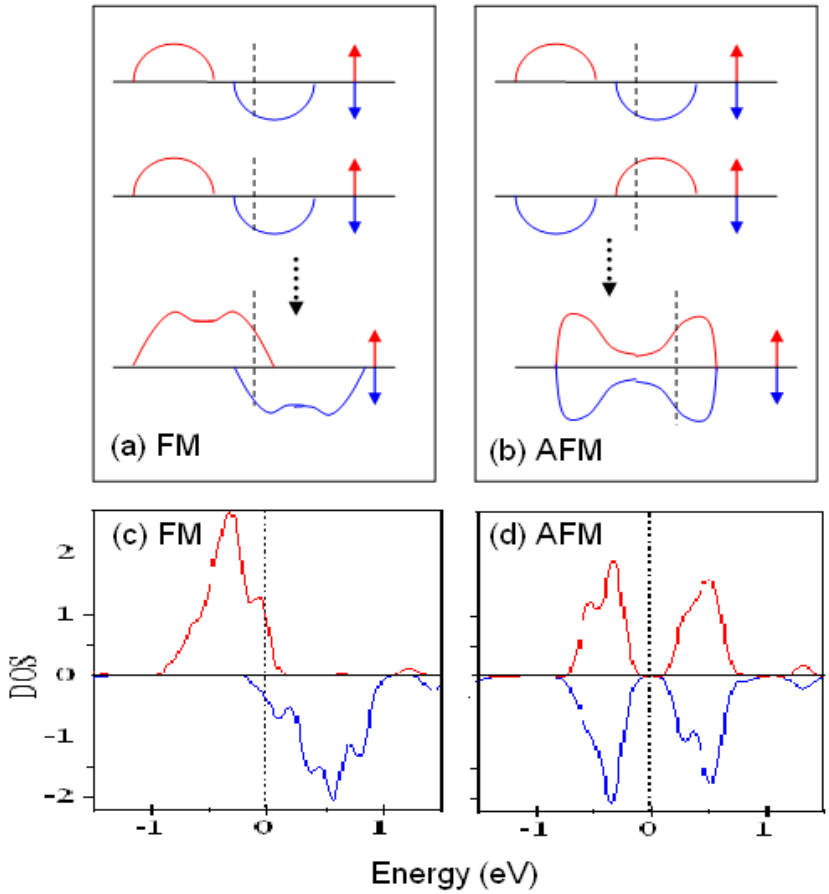

Fig. 5. (Color online) Schematic diagram of the p states coupling between them in FM (a) and AFM (b) states. The Fermi energy is indicated by the dashed vertical line. The upper side shows the DOS for two isolated B defects, and underside is the final state after the coupling for the whole system. B-2p partial DOS of FM (c) and AFM (d) state for B12 configuration calculated by GGA

Table 4. The energies difference ΔE between AFM and FM coupling, the magnetic moments of two B atoms (M_B), and the magnetic moments of the supercell (M_{SC}) for FM coupling in the case of two B spins with GGA, GGA+U_{Zn} and GGA+U_O+U_B, respectively

	Configuration (1,i)	ΔE (meV)	M_B FM (μB)	M_B AFM (μB)	M_{SC} FM (μB)
GGA	(1,2)	-87.4	0.749/0.749	0.719/-0.719	5.9745
	(1,3)	-38.4	0.748/0.748	0.731/-0.731	5.9889
	(1,4)	-131.6	0.743/0.737	0.709/-0.706	5.8564
	(1,5)	-86.3	0.749/0.749	0.719/-0.720	5.9748
GGA+U_{Zn}	(1,2)	-53.8	0.842/0.843	0.824/-0.825	6.0067
	(1,3)	-18.1	0.837/0.837	0.828/-0.828	6.0066
	(1,4)	-82.0	0.843/0.841	0.818/-0.815	6.0018
	(1,5)	-53.6	0.842/0.843	0.798/0.799	6.0067
GGA+U_O+U_B	(1,2)	-81.3	0.751/0.751	0.723/-0.725	6.0003
	(1,3)	-12.7	0.745/0.745	0.737/-0.736	6.0007
	(1,4)	-90.2	0.751/0.750	0.722/-0.721	5.9957
	(1,5)	-79.9	0.751/0.751	0.724/-0.725	6.0008

The case of two O atoms substituted by B in a supercell are investigated to study the magnetic coupling between the moments induced by B doping. We consider four different relative B-B positions in the supercell, where the first substitutional B atom is fixed at 1 site and second atom occupies the 2, 3, 4 and 5 sites, respectively, as shown in Fig. 1. The relaxed B-B distance for the four B-B positions are 4.566, 5.205, 5.628 and 7.247 Å, named B12, B13, B14 and B15 configurations. For each configuration, we perform spin-polarized GGA, GGA+U_{Zn} and GGA+U_O+U_B calculations, considering FM and AFM coupling of two B spins in the supercell respectively. The energy difference (ΔE) between AFM and FM coupling for the four configurations ($\Delta E = E^{AFM}$-E^{FM}), are listed in Table 4. ΔE is negative for all configurations, which indicates that the two B moments of B12, B13, B14 and B15 configurations are antiferromagnetically coupled. Table 4, also lists the local magnetic moments of the two B atoms for FM and AFM couplings, and the total magnetic moments of the supercell for FM coupling. Figs. 4(a) and (b), shows the spin density distribution in the relaxed supercell calculated by GGA+U_{Zn} of the B12 configuration for FM and AFM coupling. The magnetic moment induced by each B dopant and corresponding moment distribution are all

consistent with the moment and distribution in the case of isolated B substituted at O site in the supercell (see Fig. 2).

The stabilization of the FM phase observed for these systems can be understood using the phenomenological band-coupling model [57] (see Fig. 5). For the isolated B substituted at O site, the majority spin is fully occupied, whereas the minority spin is only partially occupied. In the FM phase, the 2p states with the same spin can couple to each other, forming bonding and antibonding states. The increased occupation of the spin-down bonding states stabilizes the FM phase [Fig. 5(a)]. The AFM phase is stabilized by the superexchange interaction between the occupied majority spin state on one site and the partially occupied minority spin state on the other site. The gain in energy is larger in the AFM state than in the FM state due to the second-order nature of the superexchange interaction [Fig. 5(b)], so the system is more stable in AFM phase. This is because in this case, the large coupling broadens the spin-up and spin-down band widths, causing a charge transfer from the majority spin state to the minority spin state, thus reducing the local moment and exchange splitting [Fig. 5(a)]. The reduced exchange splitting stabilizes the AFM phase, and can cause it to be the ground state. This agrees with the experiment [19] that revealed a decreasing magnetic moment per carbon as the carbon concentration increases, because the defect bands broaden as the carbon concentration increases. This model is confirmed by the DOS shown in Figs. 5(c) and (d) for GGA of B12 configuration, where indeed, both overall shape of calculated B-2p partial DOS and the corresponding occupation for the FM and AFM state agree with those predicted from the model shown in Figs. 5(a) and (b), respectively. Moreover, overall shape of calculated O-2p partial DOS near Fermi energy and the corresponding occupation for the FM and AFM state also agree with those predicted from the model.

CONCLUSION

In summary, the present study offers the following conclusions:
1. A substitution of B atom at Zn site in ZnO is non-magnetic.
2. A substitution of B atom at O site in ZnO induces magnetic moment of about 3.0 μB for GGA, GGA+U_{Zn} and GGA+U_O+U_B, respectively. And the moment mainly comes from delocalized p orbitals of B atom, its nearest neighboring Zn atoms, and its second neighboring O atoms.
3. The AFM state is the ground state for B-doped ZnO. And the GGA is more stable than the GGA+U_{Zn} and GGA+U_O+U_B calculations.
4. Partial DOS of 2p states of B atom and the corresponding occupations show that the long-range FM and AFM coupling between the magnetic moments induced by B doping can be understood from the band coupling model.
5. The addition of U_{Zn} lead DOS to downward shift of the Zn 3d states, while the DOS behavior of GGA and GGA+U_O+U_B are slightly the same.

Acknowledgments
I would like to thanks African City for Technology, Khartoum – Sudan so much.

REFERENCES

[1] J.K. Furdyna, *J. Appl. Phys.*, **1988**, 64, R29.
[2] S.A. Wolf, D.D. Awschalom, R.A. Buhrman, J.M. Daughton, S. Von Molnar, M.L. Roukes, A.Y. Chtchelkanova, and D.M.Treger, *Science*, **2001**, 294, 1488.
[3] J.F. Wager, *Science*, **2003,** 300, 124.
[4] L.–H. Ye, A.J. Freeman, and B. Delley, *Phys. Rev. B*, **2006,** 73, 033203.
[5] M. Venkatesan, C.B. Fitzgerald, J.G. Lunney, and J.M.D. *Coey*, **2004**, 93,177206.
[6] C. Sudakar, K. Padmanabhan, R. Naik, G. Lawes, B.J. Kirby, Sanjiv Kumar, and V.M. Naik, *Appl. Phys. Lett.***, 2008,** 93, 042502.
[7] Q. Xu, H. Schmidt, L. Hartmann, H. Hochmuth, M. Lorenz, A. Setzer, P. Esquinazi, C. Meinecke, and M. Grundmann, *Appl. Phys. Lett.* , **2007**, 91, 092503.
[8] K.R. Kittilstved, D.A. Schwartz, A.C. Tuan, S.M. Heald, S.A. Chambers, and D.R. Gamelin, *Phys. Rev. Lett.*, **2006,** 97, 037203.
[9] A.J. Behan, A. Mokhtari, H.J. Blythe, D. Score, X.H. Xu, J.R. Neal, A.M. Fox, and G.A. Gehring, Phys. Rev. Lett., **2008**, 100, 047206.
[10] S.K. Nayak, M. Ogura, A. Hucht, H. Akai and P. Entel, *J. Phys.: Condens. Matter.*, **2009,** 21, 064238.
[11] C.B. Fitzgerald, M. Venkatesan, L.S. Dorneles, R. Gunning, P. Stamenov, J.M.D. Coey, P.A. Stampe, R.J. Kennedy, E.C. Moreira, and U.S. Sias, *Phys. Rev. B*, **2006,** 74, 115307.
[12] A. Lussier, J. Dvorak, Y.U. Idzerda, S.B. Ogale, S.R. Shinde, R.J. Choudary, and T. Venkatesan, *J. Appl. Phys.*, **2004,** 95, 7190.

[13] J. Philip, A. Punnoose, B.I. Kim, K.M. Reddy, S. Layne, J.O. Holmes, B. Satpati, P.R. Leclair, T.S. Santos, and J.S. Moodera, *Nat. Mater.*, **2006**, 5, 298.
[14] J. Philip, N. Theodoropoulou, G. Berera, J.S. Moodera, and B. Satpati, *Appl. Phys. Lett.*, **2004**, 85, 777.
[15] C.F. Yu, T.J. Lin, S.J. Sun, and H. Chou, *J. Phys. D: Appl. Phys.*, **2007,** 40, 6497.
[16] N. H. Hong, J. Sakai, and V. Brize, *J. Phys.: Condens. Matter*, **2007,** 19,036219.
[17] Ch.F. Yu, S.H. Chen, Sh.J. Sun, and H. Chou, *J. Phys. D: Appl. Phys.*, **2009**, 42, 035001.
[18] L. Shen, R. Q. Wu, H. Pan, G. W. Peng, M. Yang, Z. D. Sha, and Y. P. Feng, *Phys. Rev. B*, **2008**, 78, 073306.
[19] H. Pan, J. B. Yi, L. Shen, R. Q. Wu, J. H. Yang, J.Y. Lin, Y. P. Feng, J. Ding, L. H. Van, and J. H. Yin, *PRL*, **2007**, 99, 127201.
[20] L. Kai, Y. Yan, W. Hongxia, Q. Zhan, Y. Sh. Mohammed and J. Hanmin, Phys. Lett. A, 374 (2010) 628.
[21] S.D. Yoon, Y. Chen, A. Yang, T.L. Goodrich, X. Zuo, D.A. Arena, K. Ziemer, C. Vittoria, and V. G. Harris, *J. Phys.: Condens. Matter*, **2006,** 18, L355.
[22] A.K. Rumaiz, B. Ali, A. Ceylan, M. Boggs, T. Beebe, and S.I. Shan, *Solid State Commun.*, 2007, 144 334.
[23] J.M.D. Coey, M. Venkatesan, and C.B. Fitzgerald, *Nature Mater.*, **2005,** 4, 173.
[24] N.A. Hill and U.V. Waghmare, *Phys. Rev. B*, **2000,** 62, 8802.
[25] V.E. Wood and A.E. Austin, Magnetoelectric Interaction Phenomena in Crystals, Gordon and Breach, New York, **1975**.
[26] P. Gopal and N.A. Spaldin, *J. Electron. Mater.*, **2006,** 35, 538.
[27] D.C. Look, J.W. Hemsky, J.R. Sizelove, *Phys. Rev. Lett.*, **1999**, 82, 2552.
[28] S.B. Zhang, S.H. Wei, A. Zunger, *Phys. Rev.*, B, **2001,** 63, 075205.
[29] S. Ghosh, V. Sih, W.H. Lau, D.D. Awschalom, S.Y. Bae, S. Wang, S. Vaidya, and G. Chapline, *Appl. Phys. Lett.*, **2005,** 86, 232507.
[30] X.L. Chen, B.H. Xu, J.M. Xue, Y. Zhao, C.C. Wei, J. Sun, Y. Wang, X.D. Zhang, X.H. Geng, *Thin Solid Films*, **2007**, 515, 3753.
[31] X. D. Liu, E. Y. Jiang, and Z. Q. Li, *Appl. Phys.*, **2007,** 102, 073708.
[32] A E Rakhshani, *J. Phys. D: Appl. Phys.*, **2008,** 41, 015305.
[33] Y. Yamamoto, K. Saito, K. Takahashi, M. Konagai, *Sol. Energy Mater. Sol. Cells*, **2001,** 65, 125.
[34] G. Kresse, J. Hafner, *Phys. Rev. B*, **1994**, 49, 14251.
[35] G. Kresse and J. Furthmüller, *Phys. Rev. B*, **1996,** 54, 11169.
[36] J. P. Perdew, K. Burke, and M. Ernzerhof, *Phys. Rev. Lett.*, **1996**, 77, 3865.
[37] V. I. Anisimov, J. Zaanen, and O. K. Andersen, *Phys. Rev. B*, **1991,** 44, 43
[38] S. L. Dudarev, G. A. Botton, S. Y. Savrasov, C. J. Humphreys, And A. P. Sutton, *Phys. Rev. B*, **1998,** 57, 1505.
[39] P. E. Blöchel, *Phys. Rev. B*, **1994,** 50, 17953.
[40] J. Monkhorst and J. Pack, *Phys. Rev. B*, **1976**, 13, 5188.
[41] P. Erhart, K. Albe, and A. Klein, *Phys. Rev. B*, **2006,** 73, 205203.
[42] A. Walsh, J.L.F. Da Silva, S.H. Wei, *Phys. Rev. Lett.*, **2008,** 100, 256401.
[43] S. Lany, H. Raebiger, A. Zunger, *Phys. Rev. B*, **2008,** 77, 241201(R)
[44] I.S. Elfimov, A. Rusydi, S.I. Csiszar, Z. Hu, H.H. Hsieh, H.J. Lin, C.T. Chen, R. Liang, and G.A. Sawatzky, *Phys. Rev. Lett.*, **2007**, 98, 137202.
[45] V. Pardo and W.E. Pickett, *Phys. Rev. B*, **2008,** 78, 134427.
[46] J. Ghijsen, L.H. Tjeng, J. van Elp, H. Eskes, J. Westerink, G.A. Sawatzky, and M.T. Czyzyk, *Phys. Rev. B*, **1988,** 38, 11322.
[47] L.H. Tjeng et al., in *Strong Correlation and Superconductivity*, edited by H. Fukuyama, S. Maekawa, and A.P. Malozemoff, Springer Series in Solid-State Sciences, Springer-Verlag, Berlin, Vol. 89, p. 85, **1989**.
[48] F. Birch, *Geophys. Res.*, **1952,** 57, 129.
[49] F. Birch, *J. Appl. Phys.*, **1938,** 9, 279.
[50] F. Birch, *Phys. Rev.*, **1947,** 71, 809.
[51] F.D. Murnaghan, *Proc. Natl. Acad. Sci. USA*, **1944,** 30, 244.
[52] J. E. Jaffe and A. C. Hess, *Phys. Rev. B*, **1993,** 48, 7903.
[53] Q. Wang, Q. Sun, G. Chen, Y. Kawazoe, and P. Jena, *Phys. Rev. B*, **2008,** 77, 205411.
[54] J. E. Jaffe, J. A. Snyder, Z. Lin, and A. C. Hess, *Phys. Rev. B*, **2000,** 62, 1660.
[55] H. Karzel, W. Potzel, M. Köfferlein, W. Schiessl, M. Steiner, U. Hiller, G. M. Kalvius, D. W. Mitchell, T. P. Das, P. Blaha, K. Schwarz, and M. P. Pasternak, *Phys. Rev. B*, **1996,** 53, 11425.
[56] S. Desgreniers, *Phys. Rev. B*, **1998,** 58, 14102.
[57] G. M. Dalpian, S.-H. Wei, X. G. Gong, A. J. R. Da Silva, and A. Fazzio, Solid State Commun., **2006**, 138, 353.